Volume 2 | Number 41 | 7 November 2014 | Pages 7085–7262

Journal of Materials Chemistry B

Materials for biology and medicine

www.rsc.org/MaterialsB

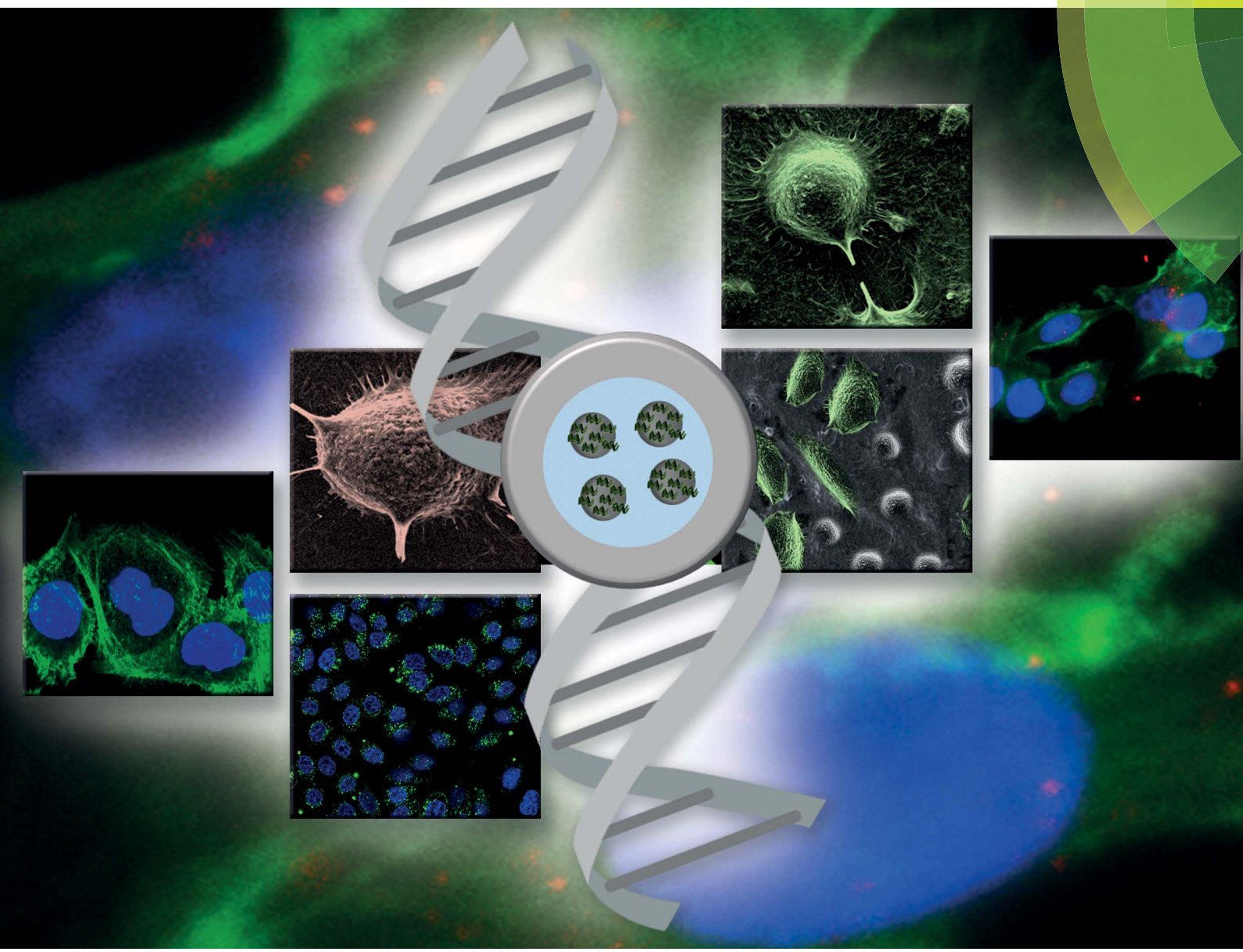

ISSN 2050-750X

ROYAL SOCIETY OF CHEMISTRY

PAPER

Matthias Epple *et al.*

A pH-sensitive poly(methyl methacrylate) copolymer for efficient drug and gene delivery across the cell membrane

Journal of Materials Chemistry B

PAPER

View Article Online
View Journal | View Issue

Cite this: J. Mater. Chem. B, 2014, 2, 7123

A pH-sensitive poly(methyl methacrylate) copolymer for efficient drug and gene delivery across the cell membrane

Gregor Doerdelmann, Diana Kozlova and Matthias Epple*

A versatile drug delivery system based on calcium phosphate/Eudragit®-E100 nanoparticles with a diameter below 200 nm was realized by a water-in-oil-in-water ($W_1/O/W_2$) emulsion solvent evaporation technique. Hydrophilic drugs (siRNA for gene silencing and bovine serum albumin as model protein) and hydrophobic drugs (5,10,15,20-tetrakis(4-hydroxyphenyl)-21*H*,23*H*-porphine, THPP, a photosensitizer for photodynamic therapy) were encapsulated as model drugs. Eudragit®-E100 is a poly(methyl methacrylate) copolymer with a low solubility at neutral pH and a high solubility at low pH. Thus, the particles are stable in cell culture media and rapidly dissolved in the lysosome after cellular uptake and delivery of their cargo into the cell. The particles had a positive charge (zeta potential +49 mV) and were taken up very well by epithelial cells (HeLa) as shown by fluorescence microscopy and confocal laser scanning microscopy. Gene-silencing experiments on HeLa-eGFP cells gave knockdown efficiencies of 39% with no toxic effects. The particles can be freeze-dried without cryoprotectant and easily redispersed in water, thus making their transport and storage convenient.

Received 29th June 2014
Accepted 26th August 2014

DOI: 10.1039/c4tb01052c

www.rsc.org/MaterialsB

Introduction

Non-viral gene therapy and vaccination with DNA, siRNA or antigens (proteins) are of continuous interest in biomedical research.[1–6] However, the administration of water-soluble and highly charged (bio-)molecules like nucleic acids for transfection or gene silencing to cells is still challenging because they not able to penetrate the cell membrane alone and also because they are subject to enzymatic degradation, *e.g.* by nucleases or proteases.[7–9] Many biomolecules find their targets inside the cell or even the nucleus,[10] therefore they have to penetrate the cell membrane.

In non-viral gene therapy, carriers like liposomes, *e.g.* 1,2-dioleoyl-3-trimethylammoniumpropane (DOTAP),[11] polyplexes of siRNA with (poly-)cationic polymers like polyethyleneimine (PEI) or nanoparticles are typically used to transport nucleic acids across the cell membrane.[6,12] Polyplexes and liposomes often show high transfection and gene silencing efficiencies, but they are also known for their cytotoxicity.[13] In contrast to polyplexes and liposomes, calcium phosphate as the inorganic part of hard tissue like bone, teeth and tendons is known for its biocompatibility and high affinity to nucleic acids.[14–20] In addition, calcium phosphate nanoparticles are efficiently taken up by cells and subsequently dissolved in lysosomes at a pH below 5.[21–26] However, due to the negative surface charge (negative zeta potential) and limited protection from nucleases (*e.g.* RNases), the transfection efficiency of such "single shell" calcium phosphate nanoparticles is typically low.[27,28]

The pharmaceutical polymer Eudragit is a copolymer, based on butylmethacrylate–(2-*N*,*N*-dimethylaminoethylmethacrylate)–methyl methacrylate (1 : 2 : 1). It is insoluble at neutral pH, but easily soluble at a pH below 5. It is mainly used for the coating of tablets to seal pH-sensitive drugs, to increase patient compliance by a better taste, and for immediate release of hydrophobic pharmaceutical ingredients in the stomach.[29,30] It is approved for pharmaceutical application. Its solubility properties open the opportunity to use it as a nanoparticulate drug and gene delivery system for the transfection of cells as nanoparticles end up in the lysosome after endocytotic uptake.[31–35] Its cationic character and solubility under acidic conditions due to the amino groups enhance the cellular uptake and the endosomal escape by the proton sponge effect.[36–40]

Earlier reports have shown that gene delivery systems based on cationic poly(2-*N*,*N*-dimethylaminoethylmethacrylate) polymers (PDMAEMA) show high transfection efficiencies with "acceptable cytotoxicity". Two parameters were found to be crucial for the high *in vitro* transfection efficiencies of PDMAEMA:[34,40,41]

1. PDMAEMA destabilizes the endosomal membrane and induces the proton sponge effect.

2. PDMAEMA dissociates easily from the nucleic acids after delivery into the cytosol.

Another problem in drug delivery is the administration of hydrophobic drugs, *i.e.* photosensitizers for photodynamic

Inorganic Chemistry and Center for Nanointegration Duisburg-Essen (CeNIDE), University of Duisburg-Essen, Universitaetsstr. 5-7, 45117 Essen, Germany. E-mail: matthias.epple@uni-due.de; Fax: +49 201 1832621; Tel: +49 201 1832402

therapy (PDT), and other BCS class II and IV drugs because their bioavailability is limited by their poor solubility in body fluids.[9,42]

Therefore, the aim of this study was to synthesize a versatile nanoparticulate drug delivery system, based on a calcium phosphate core which has been loaded before with hydrophilic or hydrophobic drugs. In addition, the Eudragit shell should protect the biomolecules from enzymatic degradation, enhance the cellular uptake by the positive particle charge, induce the proton sponge effect by amino groups, and provide a storable nanoparticulate system after freeze-drying without addition of a cryoprotectant.

Experimental

Materials

Eudragit®-E100 (denoted as Eudragit in the following) is a commercially available pharmaceutical polymer. It is a copolymer of *n*-butyl methacrylate, 2-*N*,*N*-dimethylaminoethyl methacrylate, and methyl methacrylate in a 1 : 2 : 1 molar ratio with an average molecular weight of M_w = 47 000 g mol^{-1}. It was obtained from Evonik Industries (Darmstadt, Germany) in pharmaceutical grade and used without further purification. Polyvinyl alcohol (PVA, M_w = 30 000–70 000 g mol^{-1}, 87–90% hydrolysed), fluorescein isothiocyanate-labelled bovine serum albumin (FITC-BSA, ≥7 FITC molecules per BSA molecule, M_w = ~66 kDa), herring sperm DNA (<50 base pairs), calcium-L-lactate pentahydrate (M_w = 308.31 g mol^{-1}), and di-ammonium hydrogen phosphate (M_w = 132.06 g mol^{-1}) were obtained from Sigma-Aldrich. For gene-silencing experiments with anti-eGFP-siRNA, desalted, double-stranded siRNA from Invitrogen, Ambion® (Carlsbad, USA), sense, 5′-GCAAGCUGACCCUGAA GUUCAU-3′and antisense, 5′-AUGAACUUCAGGGUCAGCUUG C-3′ (M_w = 14 019.5 g mol^{-1}) was used. All other chemicals were of analytical grade and used without further purification. All preparations were carried out with double-distilled water.

Instruments

For the formation of water-in-oil and water-in-oil-in-water emulsions, ultrasonication was carried out with a Hielscher UP50H instrument, sonotrode MS2, 70% amplitude, pulse 0.7, for 20 s. Scanning electron microscopy was performed with an ESEM Quanta 400 instrument with gold/palladium-sputtered samples. Dynamic light scattering and zeta potential determinations were performed with a Zetasizer nanoseries instrument (Malvern Nano-ZS, laser: λ = 532 nm) using the Smoluchowski approximation and taking the data from the Malvern software without further correction. The particle size data refer to scattering intensity distributions (*z*-average). Confocal laser scanning microscopy was performed with a confocal laser scanning microscope (SP5 LCSM, Leica) using a 63× water objective. The laser wavelength was 488 nm for FITC excitation (emission: 500–520 nm) and 561 nm for RFP excitation (emission: 580–600 nm). Centrifugation was performed at 4 °C with a Heraeus Fresco 21 instrument (Thermo Scientific). Gene silencing efficiencies were determined by transmission light microscopy and fluorescence microscopy with a Keyence BZ900 microscope. The viability of the cells was analysed by the MTT-test by spectrophotometric analysis with a Multiscan FC instrument (ThermoFisher scientific, Vantaa, Finland) at λ = 570 nm. Freeze-drying was performed with a Christ Alpha 2-4 LSC instrument.

Synthesis of calcium phosphate nanoparticles, loaded with anti-eGFP-siRNA

For the synthesis of calcium phosphate nanoparticles carrying anti-eGFP-siRNA, we modified the rapid precipitation method (Fig. 1) that we have reported earlier.[22,23] Aqueous solutions of calcium-L-lactate (6.25 mM, 105 μL) and $(NH_4)_2HPO_4$ (3.74 mM, 105 μL) were mixed in a Y-tube reactor with a syringe pump and pumped under continuous mixing (vortex) into an aqueous solution of anti-eGFP-siRNA (final siRNA concentration 3.3 mg mL^{-1}, 250 μL). The flow rate of both solutions was 16.6 μL s^{-1}, and the residence (nucleation) time in the Y-tube (7 mm length) was 1.3 s. After the completed precipitation, the dispersion of the nanoparticles (core: calcium phosphate; shell: siRNA) was cooled on ice and used after 5 min for the encapsulation into Eudragit nanoparticles.

Synthesis of siRNA-loaded calcium phosphate/Eudragit nanoparticles

For the encapsulation of siRNA-functionalized calcium phosphate nanoparticles into Eudragit nanoparticles, a water-in-oil-in-water ($W_1/O/W_2$) double emulsion solvent evaporation method was applied (Fig. 1). 50 μL of the dispersion of calcium phosphate/siRNA nanoparticles was added to a solution of 2 mg Eudragit, dissolved in 150 μL dichloromethane. Then, a solution of 40 μg RNase-free acetylated bovine serum albumin (BSA) in 8 μL water as dispersant was added. The mixture was immediately ultrasonicated to form the primary, milky white W_1/O-emulsion. The W_1/O-emulsion was then poured into the continuous water phase, *i.e.* 0.6 mL water with 6 mg polyvinyl alcohol (PVA) as dispersant, and ultrasonicated again.

Finally, after 3 h of vigorously stirring at room temperature, the Eudragit nanoparticles precipitated after the dichloromethane was evaporated. Thereby, the calcium phosphate nanoparticles carrying anti-eGFP-siRNA were incorporated into a nanoparticulate matrix of Eudragit. The excess of PVA was removed by centrifugation (30 min at 14 800 rpm) and redispersion of the particles in ultrapure water (three times). To determine the encapsulation efficiency of the nucleic acid, the remaining supernatant was analysed by UV/Vis spectroscopy at 260 nm according to standard protocols. The resulting dispersion was shock-frozen in liquid nitrogen and finally lyophilized at 0.31 mbar and −10 °C for 72 h. The freeze-dried particles were easily redispersable in water by gentle shaking.

Synthesis of protein-loaded calcium phosphate/Eudragit nanoparticles

Calcium phosphate/FITC-BSA/Eudragit nanoparticles were synthesized by a $W_1/O/W_2$ emulsion solvent evaporation

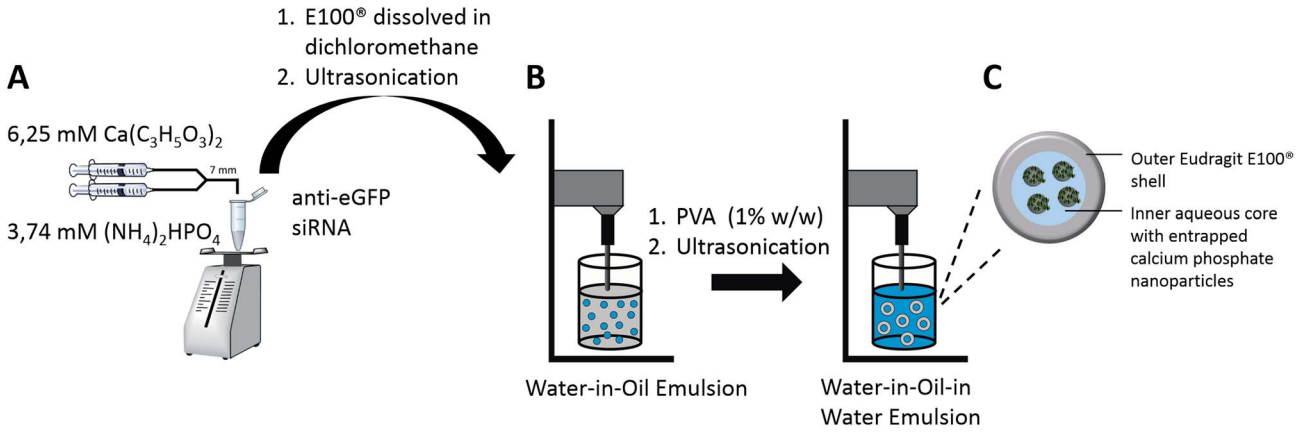

Fig. 1 Schematic pathway of the synthesis of siRNA-loaded calcium phosphate nanoparticles (A) and the encapsulation into a nanoparticulate matrix of Eudragit by a water-in-oil-in-water ($W_1/O/W_2$) double emulsion solvent evaporation method (B). Schematic representation of the particle morphology before the freeze-drying process (C).

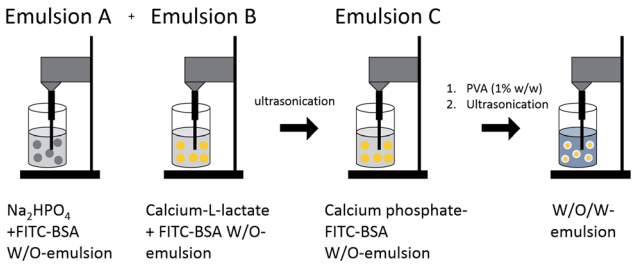

Fig. 2 Schematic pathway of the synthesis of FITC-BSA-loaded calcium phosphate/Eudragit nanoparticles.

method (Fig. 2) adopted from a synthesis reported by Tang *et al.*[43] First, two W/O emulsions (A and B) were prepared by ultrasonication. For emulsion A, 625 μg FITC-BSA was dissolved in 125 μL of a 3.74 mM solution of Na_2HPO_4. This was dispersed in a solution of Eudragit in dichloromethane (13.3 mg mL^{-1}, 375 μL). For emulsion B, 625 μg FITC-BSA was dissolved in 125 μL of a 6.25 mM solution of calcium-L-lactate. This was dispersed in a solution of Eudragit in dichloromethane (13.3 mg mL^{-1}, 375 μL). Then, emulsions A and B were mixed by ultrasonication to form emulsion C. This W_1/O-emulsion was then added dropwise to the continuous water phase (3 mL), containing 30 mg PVA as dispersant, and ultrasonicated again to form a yellow, milky $W_1/O/W_2$-emulsion. After removal of dichloromethane under reduced pressure (200–600 mbar), the calcium phosphate–FITC-BSA nanoparticles were incorporated into the nanoparticulate matrix of Eudragit. An excess of PVA and FITC-BSA was removed by centrifugation (30 min at 14 800 rpm) and redispersion of the particles in ultrapure water by ultrasonication (three times). To determine the encapsulation efficiency of FITC-BSA, the supernatants were analysed by UV/Vis spectroscopy at 460 nm after previous calibration with dissolved FITC-BSA. The resulting dispersion was shock-frozen in liquid nitrogen and finally lyophilized at 0.31 mbar and −10 °C for 72 h. The freeze-dried particles were easily redispersable in water by gentle shaking.

Synthesis of calcium phosphate/Eudragit nanoparticles, loaded with both siRNA and THPP

For the encapsulation of siRNA/calcium phosphate nanoparticles and THPP (a photosensitizer for PDT) into Eudragit nanoparticles, a water-in-oil-in-water ($W_1/O/W_2$) double emulsion solvent evaporation method was applied. First, THPP was dispersed in ethanol (4 mg in 150 μL) and added to a solution of 20 mg Eudragit in 750 μL dichloromethane. Then 150 μL of a dispersion of calcium phosphate/nucleic acid nanoparticles was added (note: for this proof of principle study, we used fragmented herring sperm DNA <50 base pairs as a model for functional siRNA at the same concentrations as for siRNA-loaded calcium phosphate nanoparticles). Then a solution of 200 μg RNase-free acetylated bovine serum albumin (BSA) in 40 μL water as dispersant was added. The mixture was immediately ultrasonicated to form the primary, milky, dark red W_1/O-emulsion. The W_1/O-emulsion was then immediately poured into the continuous water phase (3 mL), containing 30 mg polyvinyl alcohol (PVA) as dispersant, and ultrasonicated again.

Finally, the Eudragit nanoparticles were precipitated after the dichloromethane was removed under reduced pressure (200–600 mbar) in a rotary evaporator. The calcium phosphate nanoparticles carrying the nucleic acid and the hydrophobic THPP were incorporated into the nanoparticulate matrix of Eudragit. The excess of PVA was removed by centrifugation (30 min at 14 800 rpm), and redispersion of the particles in ultrapure water for three times. To determine the encapsulation efficiency of the nucleic acids and the THPP, the remaining supernatants were analysed by UV/Vis spectroscopy. The resulting dispersion was shock-frozen in liquid nitrogen and finally lyophilized at 0.31 mbar and −10 °C for 72 h. The freeze-dried particles were easily redispersable in water by gentle shaking.

Cell culture experiments

HeLa and HeLa-eGFP cells (genetically modified HeLa cells that expressed enhanced green fluorescent protein, eGFP) were

cultivated in Dulbecco's modified Eagle's medium (DMEM) supplemented with 10% fetal calf serum (FCS), 100 U mL^{-1} penicillin, and 100 U mL^{-1} streptomycin at 37 °C under 5% CO_2 atmosphere. In the case of HeLa-eGFP cells, the DMEM was additionally supplemented with geneticin (50 μg mL^{-1}). 12 h before the addition of the nanoparticles, the cells were trypsinized and seeded in 24-well plates with a density of either 2.5×10^4 cells per well (for gene silencing experiments) or 10^5 cells per well (for uptake studies).

The cell viability was analysed by the MTT-assay either for 5 h (uptake studies) or for 72 h after the treatment with nanoparticles. MTT (3-(4,5-dimethylthiazol-2-yl)-2,5-diphenyltetrazolium bromide; Sigma, Taufkirchen, Germany) was dissolved in PBS (5 mg mL^{-1}) and then poured into the required cell culture medium, giving a final MTT concentration of 1 mg mL^{-1}. The cell culture medium of transfected cells was replaced by the MTT solution (300 μL) and incubated for 90 min at 37 °C under 5% CO_2 in humidified atmosphere. Then, the MTT solution was removed and the blue precipitate was dissolved in DMSO (300 μL, each well) and incubated for 30 min. Finally, 100 μL of each well were taken for spectroscopic analysis at $\lambda = 570$ nm. The absorption of cells treated with nanoparticles was normalized to that of the control (untreated cells).

For cell uptake studies, HeLa cells were seeded in 8-well plates (BD Falcon CultureSlides, BD Biosciences Europe, Belgium) and cultivated for 24 h. Then, cells were treated with the nanoparticle dispersion (20 μL, 0.5 mg nanoparticles per mL) and examined with a confocal laser scanning microscope at different time points as described earlier.[44] For nucleic staining, the cells were incubated with 4′,6-diamidino-2-phenylindole, dilactate (DAPI, Life Technologies) for 1 h.

The gene silencing with siRNA-loaded calcium phosphate/Eudragit nanoparticles was carried out according to our protocols reported earlier.[22,45,46] Before the transfection, the cell culture medium was replaced by the nanoparticles redispersed in fresh cell culture medium (0.04 mg nanoparticles in 0.5 mL, corresponding to 3.3 μg siRNA per well). After incubation for 7 h, the transfection medium was replaced by fresh cell culture medium. As control, the cells were transfected with Lipofectamine 2000 as recommended by the manufacturer. In brief, 50 μL of FBS-free DMEM were mixed with 1 μL Lipofectamine 2000 and incubated for 5 min at room temperature. eGFP-siRNA (20 pmol, 0.28 μg) were added to 50 μL of FBS-free DMEM. Then, both solutions were mixed and incubated for 20 min before 100 μL of this solution and additionally 400 μL of DMEM were added to each well. After incubation for 7 h, the transfection medium was replaced by fresh cell culture medium. The efficiency of the gene silencing were measured 72 h after the addition of the nanoparticles by light and fluorescence microscopy.

The efficiency of the gene silencing experiments with anti-eGFP-siRNA-functionalized calcium phosphate/Eudragit nanoparticles was calculated as reported earlier:[27]

$$\frac{\text{not fluorescing cells [\%]} - \text{not fluorescing cells in control [\%]}}{\text{fluorescing cells in control [\%]}} \times 100$$

HeLa-eGFP cells cultivated under the same conditions but without any treatment were used as control.

Results and discussion

Particle size and surface charge (zeta potential) of a carrier system are important parameters that determine the ability to cross the cell membrane by endocytosis.[31,32,47,48] Furthermore, it was shown that endosomal escape mediated by the proton sponge effect and/or fusion with endosomal membranes, as well as the dissociation of the carrier material from the cargo drug inside the cytosol determine the success of the delivery system.[38–40,49] Therefore, the aim of this study was to synthesize a nanoparticulate carrier system with a diameter below 200 nm, consisting of a core of calcium phosphate nanoparticles that have a high affinity to hydrophilic biomolecules (siRNA, proteins) and a shell composed of Eudragit that protects sensitive drugs from enzymatic degradation. This additionally opens the possibility to encapsulate a hydrophobic drug inside the polymeric matrix, yielding a versatile drug delivery system. Furthermore, the cationic PDMAEMA groups in Eudragit should enhance the cellular uptake, induce the proton sponge effect, and provide the nanoparticles with a good storability.[50]

The synthesis of siRNA-loaded calcium phosphate nanoparticles was carried out according to our protocols reported earlier (Fig. 1).[22,23,27] The siRNA adsorbs on the surface of the calcium phosphate nanoparticles and inhibits their crystal growth, additionally preventing the dispersion from agglomeration by electrosteric stabilization. Thus, siRNA acts both as active pharmaceutical ingredient and as colloidal stabilization agent. For the formation of the primary W_1/O emulsion, siRNA-loaded calcium phosphate nanoparticles were dispersed in the organic phase (Eudragit dissolved in dichloromethane) by ultrasonication. This W_1/O emulsion was then added into the continuous water phase (W_2) with PVA as a stabilisation agent. Ultrasonication then led to the formation of a stable, milky-white $W_1/O/W_2$ emulsion. After evaporation of the solvent dichloromethane, the polymer precipitated and entrapped the calcium phosphate nanoparticles inside of the polymeric matrix, yielding an almost transparent nanoparticle dispersion in water.

To load the calcium phosphate nanoparticles with hydrophilic compounds that adsorb to the surface of the nanoparticles but are not able not colloidally stabilize them, the calcium phosphate nanoparticles were precipitated during the emulsion process (Fig. 2). According to the work of Landfester *et al.*, it is possible to precipitate inorganic salts in the inner aqueous droplets of primary W_1/O emulsions.[51,52] Following these lines, we have prepared two W_1/O emulsions which contained the calcium salt solution (emulsion A) and the phosphate salt solution (emulsion B) and FITC-BSA in the aqueous phase, respectively. Eudragit was dissolved in dichloromethane in the organic phase. Mixing of both emulsions under sonication led to the formation of calcium phosphate in the inner water droplets (emulsion C). Addition to the continuous water phase with PVA (1% w/w) as a stabilization agent and sonication led to the formation of a stable yellow milky $W_1/O/W_2$ emulsion. After

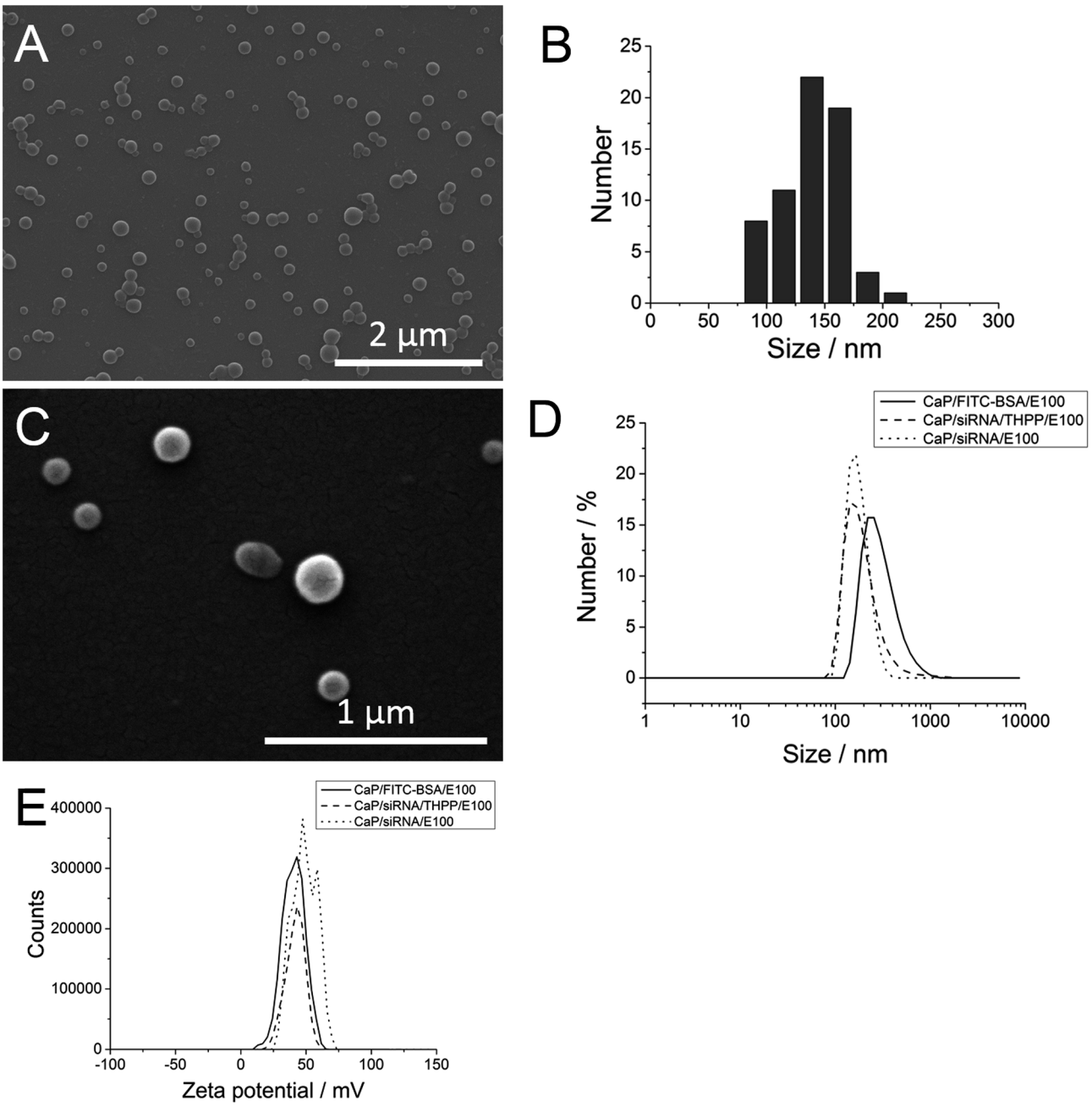

Fig. 3 Scanning electron micrograph (A) of calcium phosphate/siRNA/Eudragit nanoparticles, the corresponding particle size distribution (B), a higher-resolved scanning electron micrograph of the particles (C), size distribution curves of calcium phosphate/Eudragit nanoparticles loaded with either FITC-BSA, siRNA, or siRNA/THPP (D), and the corresponding zeta potential measurements, measured by dynamic light scattering (E).

evaporation of the solvent, the polymer precipitates and incorporates the calcium phosphate nanoparticles into the polymeric matrix, yielding an almost transparent, yellow nanoparticle dispersion.

Scanning electron micrographs of the calcium phosphate/siRNA/Eudragit nanoparticles showed spherical nanoparticles with a diameter of about 130 nm with a narrow size distribution (Fig. 3). Dynamic light scattering showed a colloidally stable nanoparticle dispersion with a polydispersity index (PDI) of 0.025, an average particle size of 198 nm (hydrodynamic diameter) and a positive zeta potential of +49 mV, indicating the successful incorporation of the anionic calcium phosphate/siRNA nanoparticles into the polycationic matrix of Eudragit with a narrow particle size distribution.

Dynamic light scattering of the calcium phosphate/FITC-BSA/Eudragit nanoparticles showed a colloidally stable nanoparticle dispersion with a polydispersity index (PDI) of 0.152, and a higher average particle size of 376 nm (hydrodynamic diameter) compared to calcium phosphate/siRNA/Eudragit nanoparticles. The zeta-potential was comparable to the siRNA-

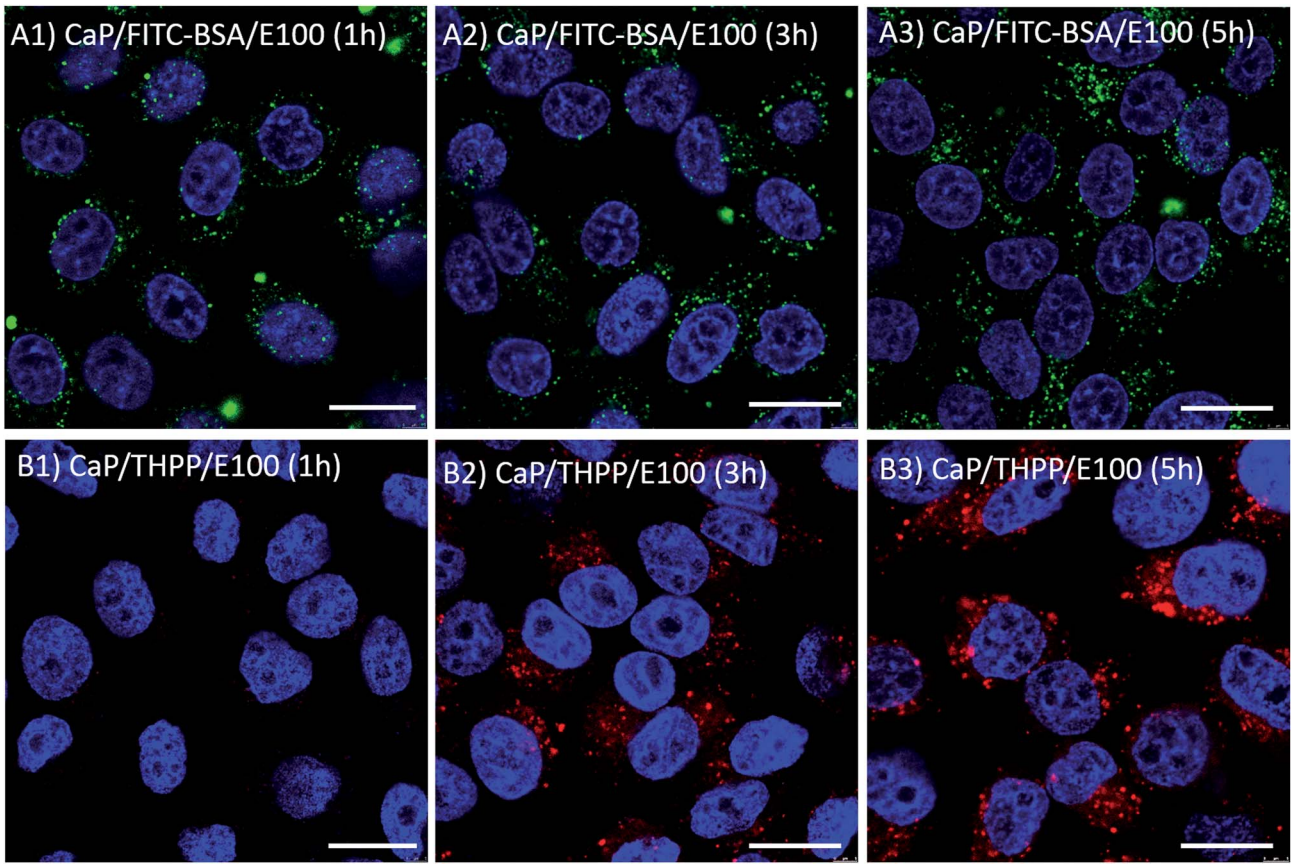

Fig. 4 Confocal laser scanning microscopy images of HeLa cells 1 h, 3 h, and 5 h after the incubation with calcium phosphate/FITC-BSA/Eudragit nanoparticles (green; A1–A3) and calcium phosphate/siRNA/THPP/Eudragit nanoparticles (red; B1–B3). The scale bar corresponds to 20 μm.

loaded nanoparticles (+40 mV), indicating the successful incorporation of the anionic calcium phosphate/FITC-BSA nanoparticles into the polymeric matrix of Eudragit (cationic) yielding calcium phosphate/FITC-BSA/Eudragit nanoparticles with a positively charged surface.

By adding a hydrophobic model drug for photodynamic therapy (THPP) to the organic phase during the synthesis procedure, we could show that this synthesis route ($W_1/O/W_2$ emulsion) is also suitable for the incorporation of hydrophobic compounds into the Eudragit matrix. With this method, we achieved high encapsulation efficiencies and high total loadings for both siRNA (100% encapsulation efficiency and 10% total loading) and for THPP (77% encapsulation efficiency and 18% total loading). Dynamic light scattering showed a similar size distribution of the calcium phosphate/siRNA/THPP/Eudragit nanoparticles compared to calcium phosphate/siRNA/Eudragit nanoparticles and a similar zeta potential (+42 mV) (Fig. 3). Note that the two peaks in the zeta potential curve for calcium phosphate/siRNA/Eudragit are probably an experimental artefact. THPP gives a red fluorescence and thereby permits to track the nanoparticles inside the cell.

Uptake studies on HeLa cells (Fig. 4) with calcium phosphate/siRNA/THPP/Eudragit and calcium phosphate/FITC-BSA/Eudragit nanoparticles showed that both types of nanoparticles are efficiently taken up by HeLa cells. The diffuse fluorescence and fine distribution of FITC-BSA and THPP inside the cytosol indicates that the nanoparticles efficiently escapes the endosomes after 3 h of incubation.

Gene-silencing experiments on HeLa-eGFP cells showed that calcium phosphate/anti-eGFP-siRNA/Eudragit nanoparticles efficiently silenced (39%) the expression of eGFP as indicated by a reduced green fluorescence (Fig. 5 and 6).

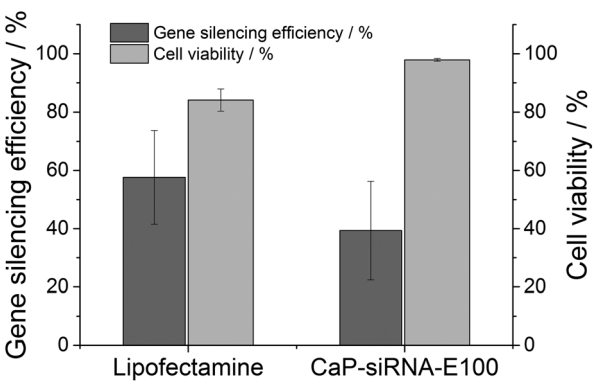

Fig. 5 Gene silencing efficiency and cell viability of HeLa-eGFP cells after the incubation with calcium phosphate/anti-eGFP-siRNA/Eudragit nanoparticles.

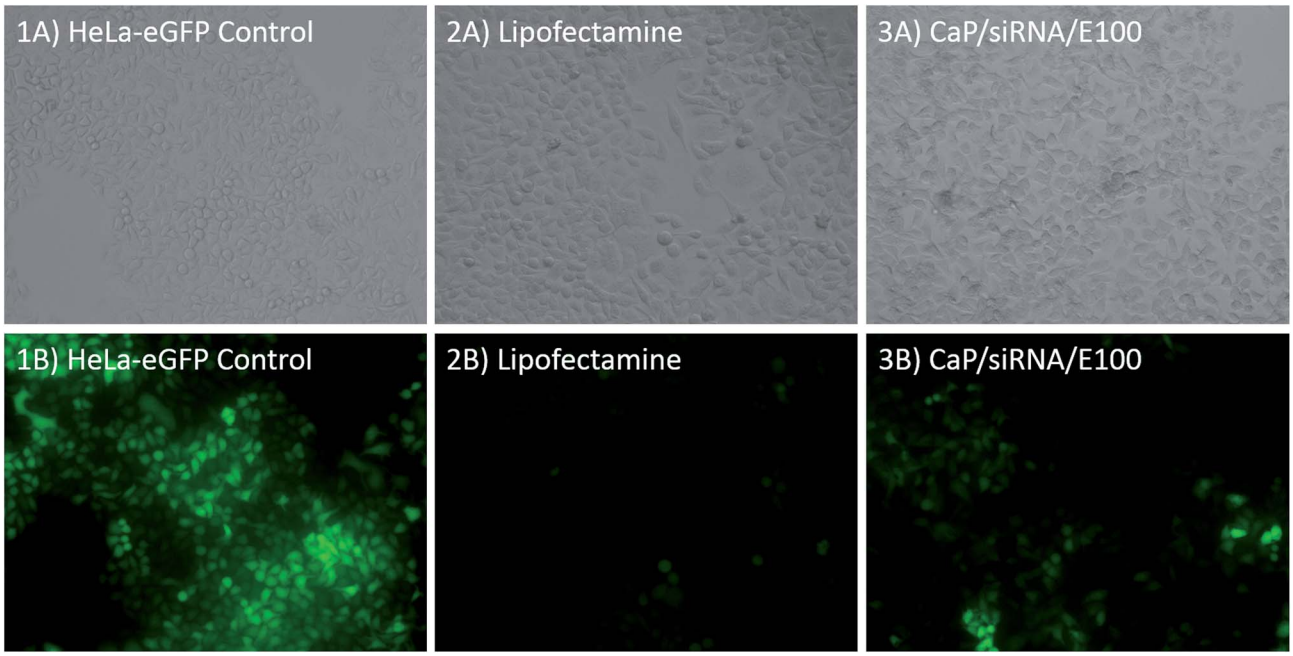

Fig. 6 Fluorescence and light microscopy images of HeLa-eGFP cells without treatment (control, 1A and 1B), after treatment with Lipofectamine (2A and 2B), and after treatment with calcium phosphate/anti-eGFP-siRNA/Eudragit nanoparticles (3A and 3B).

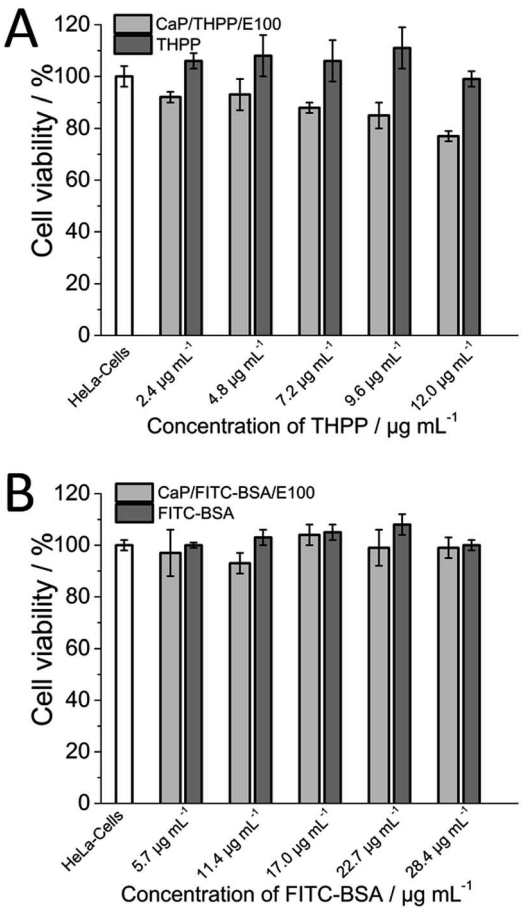

Fig. 7 Cell viability of HeLa-cells after 5 h. (A) Incubation with calcium phosphate/THPP/Eudragit (E100) nanoparticles. (B) Incubation with calcium phosphate/FITC-BSA/Eudragit (E100) nanoparticles.

To assess the toxicity of these drug delivery systems, an MTT-test was performed after 72 h of incubation of HeLa cells with calcium phosphate/anti-eGFP-siRNA/Eudragit nanoparticles (gene silencing experiments), and also after 5 h of incubation with calcium phosphate/THPP/Eudragit and calcium phosphate/FITC-BSA/Eudragit nanoparticles in different concentrations (uptake studies, Fig. 7). The results were compared to untreated HeLa cells and to cells treated with the dissolved molecules alone (FITC-BSA, THPP and Eudragit). Calcium phosphate/FITC-BSA/Eudragit nanoparticles and Eudragit nanoparticles alone showed no toxic effects up to a final concentration of 0.1 mg mL^{-1} in the cell culture medium. Calcium phosphate/THPP/Eudragit nanoparticles were slightly more toxic than THPP (dissolved in ethanol) alone. As THPP is toxic at higher concentrations,[45,53] this toxic effect can be explained with an enhanced cellular uptake induced by the nanoparticles.

Conclusions

We have demonstrated that calcium phosphate/Eudragit nanoparticles are a versatile drug and gene delivery system for both hydrophilic and hydrophobic drugs, *i.e.* siRNA, FITC-BSA and siRNA/THPP. The resulting particles had a diameter of about 130 nm size and a highly positive surface charge. They were efficiently taken up by HeLa cells and escaped the endosomes after 3 h of incubation. Toxicity studies showed that calcium phosphate/Eudragit nanoparticles are not cytotoxic up to a concentration of 0.1 mg mL^{-1} after 5 h of incubation. The particles can be easily freeze-dried for better storage without a cryoprotectant and easily redispersed in water. We conclude that calcium phosphate/Eudragit nanoparticles represent a

versatile drug delivery system for biomolecules and synthetic molecules, adapted to the requirements for good cellular uptake and endosomal escape.

Acknowledgements

We thank the Deutsche Forschungsgemeinschaft (DFG) for financial support of this project (Ep 22/35-1). We thank Prof. Shirley Knauer, University of Duisburg-Essen, for access to the confocal laser scanning microscope.

References

1 C. X. Li, A. Parker, E. Menocal, S. Xiang, L. Borodyansky and J. H. Fruehauf, *Cell Cycle*, 2006, **5**, 2103–2109.
2 L. De Laporte, J. Cruz Rea and L. D. Shea, *Biomaterials*, 2006, **27**, 947–954.
3 F. D. Ledley, *Curr. Opin. Biotechnol.*, 1994, **5**, 626–636.
4 G. Gregoriadis, *Curr. Opin. Mol. Ther.*, 1999, **1**, 39–42.
5 M. A. Kutzler and D. B. Weiner, *Nat. Rev. Genet.*, 2008, **9**, 776–788.
6 J. Kurreck, *Angew. Chem., Int. Ed.*, 2009, **48**, 1378–1398.
7 M. S. Shim and Y. J. Kwon, *FEBS J.*, 2010, **277**, 4814–4827.
8 J. Wang, Z. Z. Lu, M. G. Wientjes and J. L. S. Au, *AAPS J.*, 2010, **12**, 492–503.
9 G. L. Amidon, H. Lennernaes, V. P. Shah and J. R. Crison, *Pharm. Res.*, 1995, **12**, 413–420.
10 G. L. Verdine and L. D. Walensky, *Clin. Cancer Res.*, 2007, **13**, 7264–7270.
11 C. G. Oster, N. Kim, L. Grode, L. Barbu-Tudoran, A. K. Schaper, S. H. E. Kaufmann and T. Kissel, *J. Controlled Release*, 2005, **104**, 359–377.
12 V. Sokolova and M. Epple, *Angew. Chem., Int. Ed.*, 2008, **47**, 1382–1395.
13 H. T. Lv, S. B. Zhang, B. Wang, S. H. Cui and J. Yan, *J. Controlled Release*, 2006, **114**, 100–109.
14 V. Uskokovic and D. P. Uskokovic, *J. Biomed. Mater. Res., Part B*, 2011, **96**, 152–191.
15 M. Epple, K. Ganesan, R. Heumann, J. Klesing, A. Kovtun, S. Neumann and V. Sokolova, *J. Mater. Chem.*, 2010, **20**, 18–23.
16 Y. Cai and R. Tang, *J. Mater. Chem.*, 2008, **18**, 3775–3787.
17 Z. P. Xu, Q. H. Zeng, G. Q. Lu and A. B. Yu, *Chem. Eng. Sci.*, 2006, **61**, 1027–1040.
18 A. Maitra, *Expert Rev. Mol. Diagn.*, 2005, **5**, 893–905.
19 J. C. Le Huec, D. Clement, E. Lesprit and J. Faber, *Eur. J. Orthop. Surg. Traumatol.*, 2000, **10**, 223–229.
20 M. Bohner, *Injury*, 2000, **31**(suppl. 4), D37–D47.
21 A. E. Ewence, M. Bootman, H. L. Roderick, J. N. Skepper, G. McCarthy, M. Epple, M. Neumann, C. M. Shanahan and D. Proudfoot, *Circ. Res.*, 2008, **103**, e28–e32.
22 S. Neumann, A. Kovtun, I. D. Dietzel, M. Epple and R. Heumann, *Biomaterials*, 2009, **30**, 6794–6802.
23 V. Sokolova, D. Kozlova, T. Knuschke, J. Buer, A. M. Westendorf and M. Epple, *Acta Biomater.*, 2013, **9**, 7527–7535.
24 Y. Dautova, D. Kozlova, J. N. Skepper, M. Epple, M. D. Bootman and D. Proudfoot, *PLoS One*, 2014, **9**, e97565.
25 O. Rotan, V. Sokolova, P. Gilles, W. Hu, S. Dutt, T. Schrader and M. Epple, *Materialwiss. Werkstofftech.*, 2013, **44**, 176–182.
26 V. Sokolova, O. Rotan, J. Klesing, P. Nalbant, J. Buer, T. Knuschke, A. M. Westendorf and M. Epple, *J. Nanopart. Res.*, 2012, **14**, 910.
27 V. Sokolova, A. Kovtun, O. Prymak, W. Meyer-Zaika, E. A. Kubareva, E. A. Romanova, T. S. Oretskaya, R. Heumann and M. Epple, *J. Mater. Chem.*, 2007, **17**, 721–727.
28 V. Sokolova, S. Neumann, A. Kovtun, S. Chernousova, R. Heumann and M. Epple, *J. Mater. Sci.*, 2010, **45**, 4952–4957.
29 M. M. Patel and A. F. Amin, *J. Pharm. Sci.*, 2011, **100**, 1760–1772.
30 P. Roy and A. Shahiwala, *J. Controlled Release*, 2009, **134**, 74–80.
31 I. Canton and G. Battaglia, *Chem. Soc. Rev.*, 2012, **41**, 2718–2739.
32 T. G. Iversen, T. Skotland and K. Sandvig, *Nano Today*, 2011, **6**, 176–185.
33 G. Sahay, D. Y. Alakhova and A. V. Kabanov, *J. Controlled Release*, 2010, **145**, 182–195.
34 M. Gargouri, A. Sapin, S. Bouali, P. Becuwe, J. L. Merlin and P. Maincent, *Technol. Cancer Res. Treat.*, 2009, **8**, 433–443.
35 W. N. Haining, D. G. Anderson, S. R. Little, M. S. von Bergwelt-Baildon, A. A. Cardoso, P. Alves, K. Kosmatopoulos, L. M. Nadler, R. Langer and D. S. Kohane, *J. Immunol.*, 2004, **173**, 2578–2585.
36 A. Basarkar and J. Singh, *Pharm. Res.*, 2009, **26**, 72–81.
37 M. X. Tang and F. C. Szoka, *Gene Ther.*, 1997, **4**, 823–832.
38 P. Dubruel, J. De Strycker, P. Westbroek, K. Bracke, E. Temmerman, J. Vandervoort, A. Ludwig and E. Schacht, *Polym. Int.*, 2002, **51**, 948–957.
39 P. Dubruel, B. Christiaens, M. Rosseneu, J. Vandekerckhove, J. Grooten, V. Goossens and E. Schacht, *Biomacromolecules*, 2004, **5**, 379–388.
40 P. Dubruel, B. Christiaens, B. Vanloo, K. Bracke, M. Rosseneu, J. Vandekerckhove and E. Schacht, *Eur. J. Pharm. Sci.*, 2003, **18**, 211–220.
41 S. K. Samal, M. Dash, V. S. Van, D. L. Kaplan, E. Chiellini, C. A. van Blitterswijk, L. Moroni and P. Dubruel, *Chem. Soc. Rev.*, 2012, **41**, 7147–7194.
42 C. Wischke and S. P. Schwendeman, *Int. J. Pharm.*, 2008, **364**, 298–327.
43 J. Tang, J. Y. Chen, J. Liu, M. Luo, Y. J. Wang, X. W. Wei, X. Gao, B. L. Wang, Y. B. Liu, T. Yi, A. P. Tong, X. R. Song, Y. M. Xie, Y. Zhao, M. Xiang, Y. Huang and Y. Zheng, *Int. J. Pharm.*, 2012, **431**, 210–221.
44 S. Tenzer, D. Docter, J. Kuharev, A. Musyanovych, V. Fetz, R. Hecht, F. Schlenk, D. Fischer, K. Kiouptsi, C. Reinhardt, K. Landfester, H. Schild, M. Maskos, S. K. Knauer and R. H. Stauber, *Nat. Nanotechnol.*, 2013, **8**, 772–781.
45 J. Klesing, A. Wiehe, B. Gitter, S. Gräfe and M. Epple, *J. Mater. Sci.: Mater. Med.*, 2010, **21**, 887–892.

46 V. Sokolova, A. Kovtun, R. Heumann and M. Epple, *J. Biol. Inorg. Chem.*, 2007, **12**, 174–179.
47 K. Sandvig, S. Pust, T. Skotland and B. van Deurs, *Curr. Opin. Cell Biol.*, 2011, **23**, 413–420.
48 H. Hillaireau and P. Couvreur, *Cell. Mol. Life Sci.*, 2009, **66**, 2873–2896.
49 A. K. Varkouhi, M. Scholte, G. Storm and H. J. Haisma, *J. Controlled Release*, 2011, **151**, 220–228.
50 C. Vauthier and K. Bouchemal, *Pharm. Res.*, 2009, **26**, 1025–1058.
51 A. Hamberger, U. Ziener and K. Landfester, *Macromol. Chem. Phys.*, 2013, **214**, 691–699.
52 N. Nabih, K. Landfester and A. Taden, *J. Polym. Sci., Part A: Polym. Chem.*, 2011, **49**, 5019–5029.
53 J. Schwiertz, A. Wiehe, S. Gräfe, B. Gitter and M. Epple, *Biomaterials*, 2009, **30**, 3324–3331.